Research Project and Seminar

Informatik-Ingenieurwesen

Orthogonal Codes for Acoustic UnderwaterLocalization

by

Sergej Keller

April 2022

Supervised by

Christoph Weyer
Institute of Telematics, Hamburg University of Technology

First Examiner | Prof. Dr.-Ing. Bernd-Christian Renner
Institute of Autonomous Cyber-Physical Systems
Hamburg University of Technology

Second Examiner | Prof. Dr. Volker Turau
Institute of Telematics
Hamburg University of Technology

Institute of Autonomous Cyber-Physical Systems
Hamburg University of Technology

TUHH

Table of Contents

Chapter 1

Introduction

Acoustic signals are nowadays mostly used for military and research propose. Electromagnetic waves cant perpetuate water, so by the use of acoustic modems water can be used as a medium. Underwater vehicles need to be capable of communicate to either themselves or objects placed at the surface. Even though the throughput of these acoustic signals is way less than its electromagnetic counterpart, it still has the advantage to perpetuate fluids.

1.1 Motivation

Using water as a medium for localization signals can be somewhat sophisticated to implement and are therefore a challenging research topic. Due strong damping of the classic electromagnetic waves general technologies like GPS or GLONAS are not applicable in under water scenarios.

Acoustic transmission comes in handy in this case. Most systems use a vehicle which transmits acoustic beacons. These are then received by hydrophones placed at the surface. By estimating the travel times the distance between hydrophones and the underwater vehicle can be calculated. However, to let it localize itself, the reverse method is needed. Thus, anchors firmly fixed at the surface send their individual signals and the vehicle receives them.

Signals send by the anchors need to be separable but still observable. Therefore we need codes that are orthogonal towards each other but nonetheless posses clear auto-correlation.

This project dives into the mathematical details of pseudo.random maximum length sequence generation and signal processing. By the use of cross-correlation and auto-correlation the separation of signals can be implemented and evaluated. USB-Oscilloscope

1.2 Setup

The initial Setup is made of two acoustic anchors placed at a footbridge. An acoustic receiver connected to a USB-Oscilloscope is placed between them.

The advanced setup consists of 4 Anchors fixed at the surface broadcasting different signals produced from an python program. Acoustic Modems use broadcast the transfer band signal into the water. At the beginning these 4 anchors need to be synchronized. A blueROV2 receives these signals under water and saves them. Afterward the saved signals are used in python to calculate the position of the ROV.

Figure 1.1: BlueROV2 from Blue Robotics Inc

1.3 Principle

To get the appropriate signals we need to apply certain signal processing steps. First the pseudo-random codes gets up-sampled and put though an cosine FIR filter to remove high frequencies from the base-band. The resulting signal is than shifted to the transfer band. Hereon either a custom delay is artificially added by zero padding for the simulation or is send by the acoustic modem.

Because of the advantageous properties of the used codes the different codes can be separated by cross-correlation by the not delayed versions. The cleaner the auto-correlation the higher are the peaks which are used to measure the initial delay. Method of peak detection may needed to filter out peaks caused from reflections.

Chapter 2

PN and orthogonal sequences

To attain a higher level of localization accuracy, there are two primary goals that must be pursued.

First, the code used for underwater localization should have an auto-correlation function that approaches a Dirac impulse. This is important because it allows for more efficient detection through the use of correlation techniques.

The second factor to consider is the cross-correlation properties of the code. It is essential that these attributes meet certain criteria in order to improve separation from other sequences. Mathematically speaking, this means that the codes should be orthogonal to each other, or at least approaching orthogonality. This will be particularly useful in real-world scenarios where noise, reflections, and other artifacts may be present.

In summary, by striving to achieve both of these objectives, it is possible to significantly improve the localization accuracy.

2.1 Pseudo-random codes

There are a couple of techniques to generate PN sequences. Most of these methods use linear feedback shift registers to generate the codes by an initial condition or seed value. In this project I will concertize my research on gold codes, kasami codes and the basic m-sequences which are used for generating gold codes. These types are all based on linear shift registers.

M-sequences are defined as binary PN codes, which are generated by linear shift registers with feedback. The sequences are periodic, and contain an equal number of zeros and ones [PS08]. Maximum length sequences need to fulfill certain criteria. First its length is defined by $N = 2^n - 1$ where n is the maximum degree of the generator polynomial $f(X)$ [SP80].

$$|u| = 2^n - 1 = N, \quad \text{from polynomial } h(x) \text{of degree } n \tag{2.1}$$

$$\frac{N}{gcd(N,q) = N}, \quad \text{from decimation polynomials } \widetilde{h(x)} \tag{2.2}$$

Second the cross-correlation between m-sequences must take three values only, which are -1, $-t(n)$, $t(n) - 2$. With it $t(n)$ is defined by $1 + 2^{\lfloor 0.5(n+2) \rfloor}$ [SP80]. If every pair of m-sequences is a preferred pair, they form a maximal connected set and these sets have a limited carnality. Experiments from Gold and Koptizke showed that the number of such connected pairs is limited. Between degrees

[GK65]. To get an m-sequence we need a primitive polynomial.

2.1.1 Gold Codes

Because of not optimal cross-correlation properties m-sequences alone are not applicable for the project. But if these type of codes are combined their correlation qualities can change. Gold Codes are m-sequences where two of them with same length are modulo-2 summed. [PS08]

Recent research shows that some gold codes have high similarity to a Gaussian random variable [MD].

$$Gold(u,v) = \{u, v, u \oplus v, u \oplus (v \ll 1), \ldots, u \oplus (v \ll N-1)\} \tag{2.3}$$

2.1.2 Kasami Codes

Kasami sequences are constructed in the similar fashion by using m-sequences with the exception that a second sequence, which is used in the modulo sum, is formed by decimating the default m-sequence by $2^{m/2}$ [PS08] [SP80] [PPWW72]. Thus, only one generator polynomial is required.

$$w = u[2^{N/2} + 1] = \{u_1, \ldots, u_i, \ldots, u_N | \text{take every } i\text{-th bit of u}\} \tag{2.4}$$

$$Kasami(u) = \{u, u \oplus w, u \oplus (w \ll 1), \ldots, u \oplus (w \ll 2^{N/2} - 2)\} \tag{2.5}$$

2.2 Comparison

For the localization process by orthogonal codes certain criteria needs to be met, which were named in the first chapter. To compare the before explained code types two measures are introduced.

The first one is the peak to side-lobe ratio (PSR) 2.6. This measure is defined by subtracting the mean from the peak of the auto-correlation. Then this value get divided by the standard deviation of the same auto-correlation. A higher PSR value signifies a lower error between the auto correlation and the perfect Dirac resulting in better detection capability. The second one is the ratio between the auto-correlation peak and the maximum of the cross-correlation (ACR) 2.7. There a higher value indicates good code separation qualities.

The comparison is done by sampling pairs at degrees six to ten N times from the set of random sequences. These pairs are then used for generating the wanted pseudo-random codes like gold or kasami. Afterwards for all three code types the shown measures are applied.

$$PSR = \frac{max\{x_{ac}\} - \overline{x_{ac}}}{\sigma_{ac}} \tag{2.6}$$

$$ACR = \frac{max\{x_{ac}\}}{max\{x_{cc}\}} \tag{2.7}$$

In this evaluation of data, three types of codes were compared. Maximum length sequences, Gold Codes, and Kasami Codes. The performance of each code was assessed using two ratios, the ACR and the PSR.

From preferred polynomial all possible maximum length sequences, gold sequences and kasami sequences are generated. Then both measures are applied on the cross-correlation and auto-correlation functions of the random codes. The PSR and ACR measures are plotted against the used polynomials. Also the best case of PSR and ACR are plotted by their given correlation function.

Maximum length sequences hold the best auto-correlation properties in comparison to its competitors. But it shows peaks in its cross-correlation, making it a rather bad option for orthogonal separation. The kasami sequence has a way better cross-correlation but still a small peak. The clear winner are gold codes because of the good auto-correlation and very good cross-correlation properties 2.3. Its auto-correlations lags a bit behind its competitors but orthogonality is as much as important.

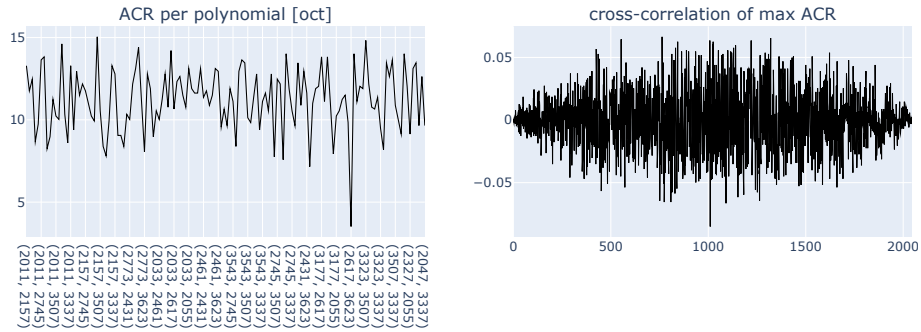

Figure 2.1: Evaluation of gold sequences by AC ratio

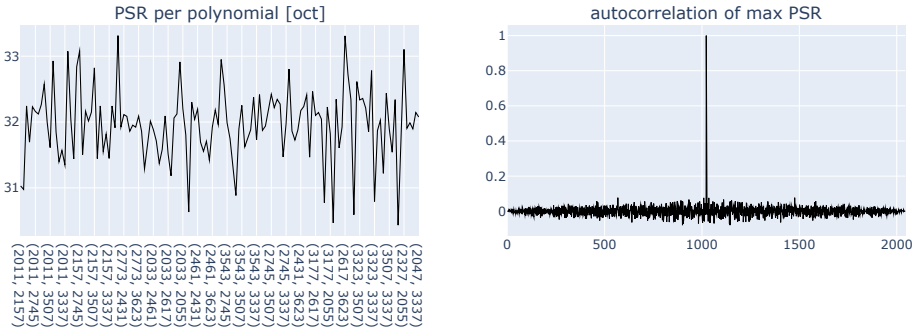

Figure 2.2: Evaluation of gold sequences by PS ratio

To get more valuable data, elements from each set of codes are sampled uniformly ($N = 1000$) and afterwards the evaluation parameters are applied. The results yields that Gold Codes had the least increase in PSR, but were the second best at ACR. Kasami Codes were only slightly better in both PSR and ACR than Gold Codes, but had a smaller set of codes available. Maximum length sequences had the highest PSR, but the worst ACR.

Based on these findings, it can be concluded that Gold Codes are the best choice for this application. While maximum length sequences had the highest PSR, they performed poorly in terms of ACR. Gold Codes, on the other hand, had a good balance of performance in both ratios, and also had a large set of codes available. In addition, Gold Codes demonstrated better cross-correlated detection compared to maximum length sequences.

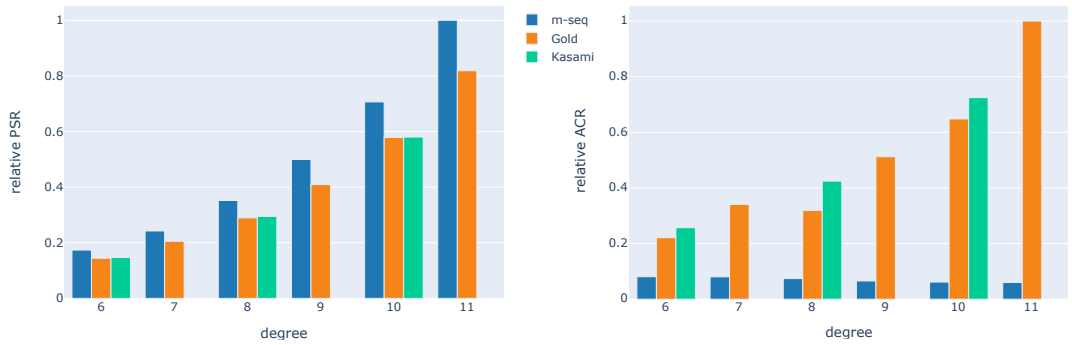

Figure 2.3: Evaluation by relative PSR for degrees 6 to 11

Chapter 3

Signal Processing

After code generation the binary data needs to be transormed into a transmittable signed signal

3.1 Pulse shaping

The raw code which was previously generated is first put through an sign function, which sets its mean to zero. The discontinuous signal holds an infinite bandwidth because it consists of rectangular pulses. These pulse spans have infinity frequency, which are impossible to implement for acoustic transmission. Therefore a restriction to a certain bandwidth must be introduced. Such a reduction is possible by applying an low-pass filter.

Because limiting the signals bandwidth introduces a damped oscillation, which leads to incorrect decoding of received data [Gen07], a appropriate choice of filter would be a the raised cosine 3.1. Such a pulse filter is defined by a squared cosine, which decreases its amplitude in frequency. In our case the roll off factor α is set to 0.125 and symbol length T_{sym} to the inverse of our target bandwidth $20\,kHz$.

Before applying the filter the generated codes need to be up-scaled for our target sampling rate. The relation between sampling rate f_s and up-sampling factor Sp_s is $Sp_s = fs \cdot T_{sym}$.

$$H(\omega) = T_{sym} \cdot \cos^2\left(\frac{T_{sym}(\omega - \pi(1-\alpha)/T_{sym})}{4\alpha}\right), \quad \omega = 2\pi f \tag{3.1}$$

3.2 Shift to Carrier

Now that our base band signal $tSigBB[k]$ has its target bandwidth and sample rate only the frequency shift to the carrier frequency f_c of $62.5\,kHz$ is necessary. That procedure is accomplished by multiplying our sampled signal by the exponential function, where f_c is passed to its exponent. An Frequency shift of the transmitted signal can be achieved by multiplying it with a complex exponential function of the form $e^{-2\pi j f_c k}$. This results in a

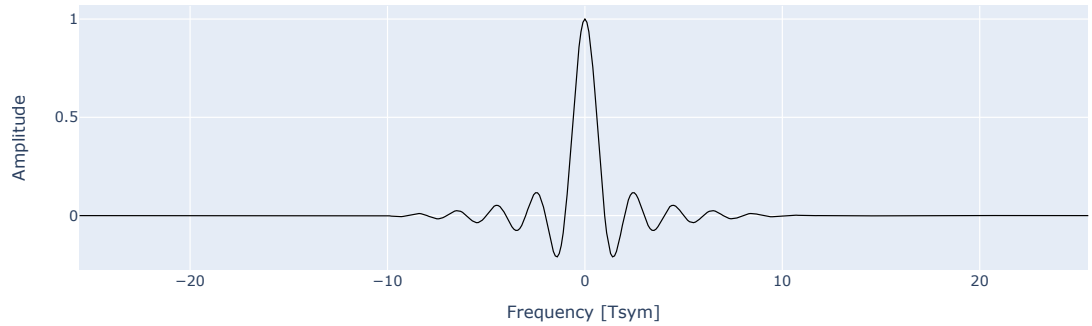

Figure 3.1: Section of Cosine FIR with a resolution of 1024

phase rotation in the frequency domain and effectively shifts the spectrum of the signal by f_c. The resulting signal could hold imaginary parts, hence only the real part is passed through for transmission.

The signal is now in an almost appropriate state for the use inside an localization algorithm, where the delays of the signals can be detected by the help of cross-correlation techniques.

$$x_{tSigTB}[k] = Re\{x_{tSigBB}[k] \cdot e^{-2\pi j f_c k}\} \tag{3.2}$$

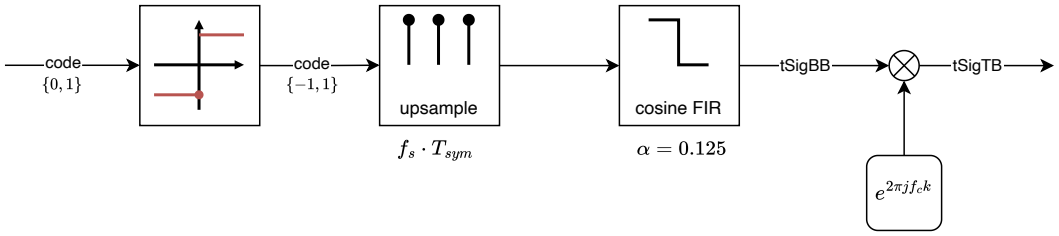

Figure 3.2: Processing of generated signal

3.3 Band pass filter

On the receiver side all signals are received as a sum, which is mixed by artifacts of signal reflections and random noise from the electronics.

The received signal may also have noise around its bandwidth because of its frequency shift. Thus, we only pass though frequencies inside our frequency band by applying a butterworth band pass filter. A flat magnitude is favorable because only frequencies of the base-band should be passed through. The filter gets applied after shifting back to the base-band. Such a filter, namely a maximally flat magnitude filter, approximates this goal. The roll-off decreases by increasing the order of the system.

The critical frequencies of the applied filter are $f_c \pm \frac{bw}{2}$ by an Order of 5. Thus frequencies get removed which are not inside the spectrum of interest. To remove shifts in time the filter is applied forwards and backwards following a doubling of its order. By using the filter twice the order gets doubled.

3.4 Shift to base band

Shifting the transmitted signal back to its original frequency is feasible by just changing its sign. In this case also the imaginary part can be retained.

$$x_{tSigBB}[k] = x_{tSigTB}[k] \cdot e^{2\pi j f_c k} \tag{3.3}$$

3.5 Low-pass Filter

Because of spectral noise resulting from the base band shift could result in worse peak detection capabilities, the same kind of filter, which was used for pruning the carrier frequencies is used as a low-pass. The same Order and twice filtering principle is used.

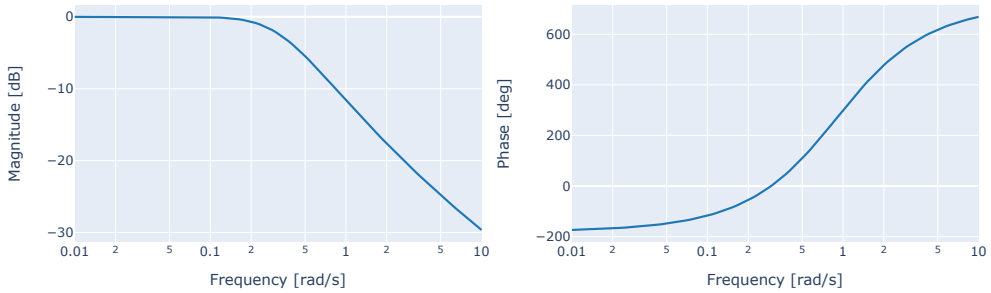

Figure 3.3: Bode plot of 5th order Butterworth low-pass filter

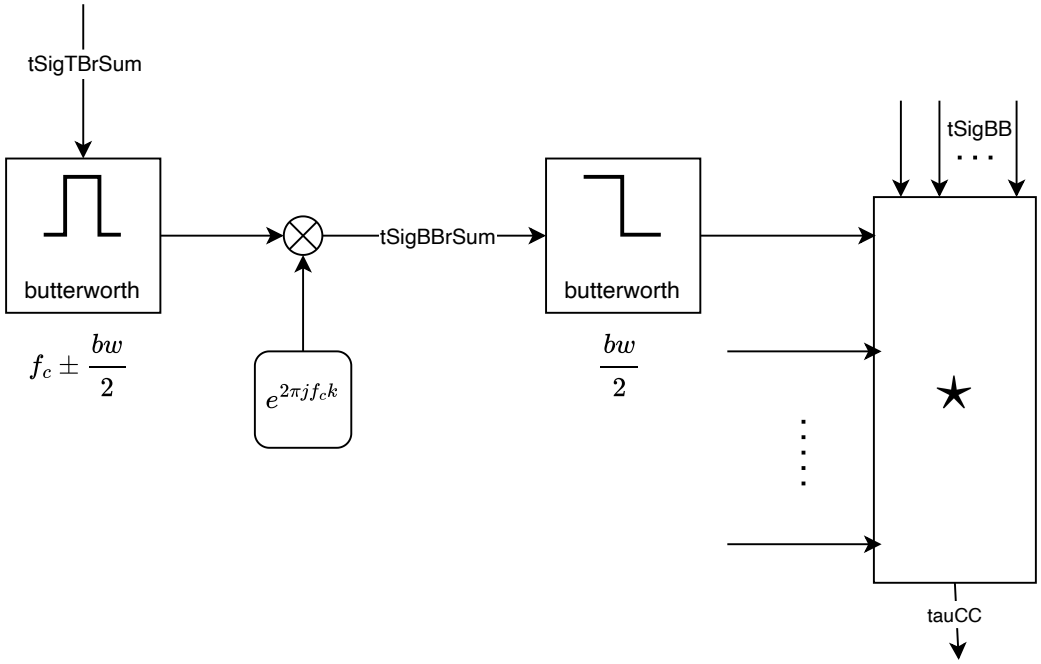

Figure 3.4: Processing of received signal

Chapter 4

Simulation

The simulation consists of a watermark benchmark [vWOJ] and a SNR driven Gaussian white noise added to the sum of the signals.

4.1 Watermark

The Watermark Simulation consists of a convolution or channel replay by an selected channel TVIR estimate. The channels consist of multiple dirac impulses of different strengths. Thus, reflections and reduced signal strength are simulated.

$$x_{tSigTBr}[k] = \sum_{i=0}^{N} h[k,i] \cdot x_{tSigTB}[k-i] \tag{4.1}$$

4.2 White Noise

A additive Gaussian White Noise (GWN) generated by a desired Signal to Noise Ratio (SNR) between $-20dB$ and $20dB$ in steps of $5dB$. From the general equation of the Signal to Noise Ratio we derive our noise standard deviation by transforming this ratio. The white noise is added after the simulation and before receiver filtering. To estimate the power of our signal a standard deviation estimation is used, which consists of all incoming signals by using its expected value. The Gaussian noise is generated by using a normal distributed random variable with its mean at zero and its standard deviation at $\frac{\bar{\sigma}}{SNR}$. Thus, M denotes the number of total anchors and N is the length of the corresponding signal.

$$\bar{\sigma} = \frac{1}{M}\sum_{i=0}^{M}\sigma_i, \quad \sigma_j = \sum_{k=0}^{N} tSigTBr_j{}^2[k] \tag{4.2}$$

$$n[k] = f_{GWN}[k] \cdot \frac{\bar{\sigma}}{SNR}, \quad GWN \sim \text{Normal}(0,1) \tag{4.3}$$

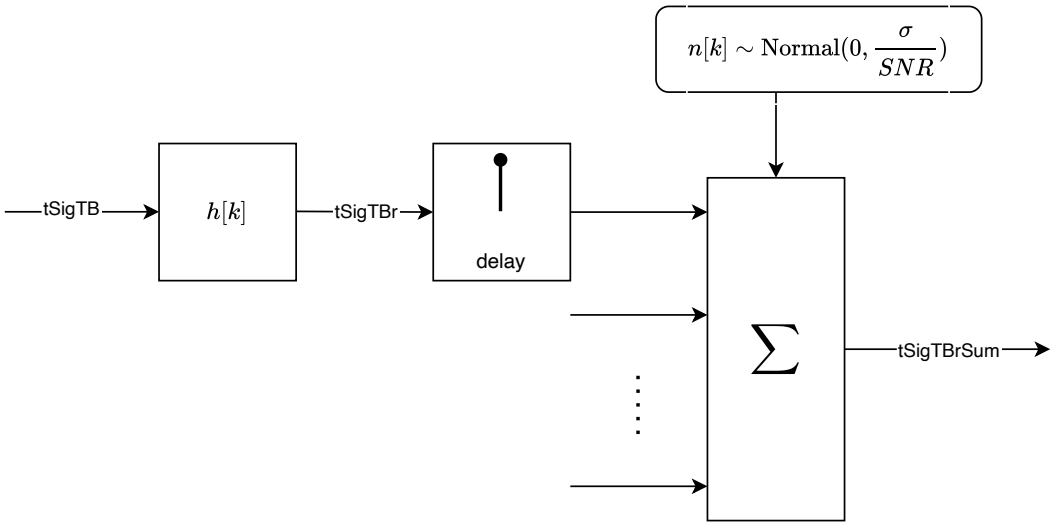

Figure 4.1: Simulation of acoustic signal propagation

Chapter 5

Localization

5.1 Peak detection

The received signal, consisting of summed delayed signals, cross-correlated by every anchor. If the signal is not reflected the peak in cross-correlation would be obvious. But because by the introduction of noise and water reflections a higher rate of similar peaks appear. To suppress these effects a CA-FAR Algorithm [Roh11] is applied to only detect the first reflected peak resulting in lower false alarms of peaks.

CA-FAR works by using multiple values intervals. The most outer one could be described as a train bin and is used to get an estimation of the signals noise. Especially CA-FAR uses averaging to estimate the noise by measured cells. The bordering bin, defined as the guard cells, is used to reduce self-interference of the peaks. Thus, increasing window sizes W results in better noise estimating but overall detectability is still limited by the sample rate [Roh11][rad]. By knowledge of measured peak widths a optimal guard interval can be figured.

The calculated threshold is than scaled by factor S depending on a formula based on the false alarm rate η. The higher the false alarm rate, the weaker high amplitude peaks gets included by the estimated threshold 5.1.

$$S = 2W\left(\eta^{-1/2W} - 1\right) \tag{5.1}$$

$$T = S \cdot Z, \quad Z_{CA} = \sum_{i=1}^{W} \frac{1}{W} x_{train} \tag{5.2}$$

5.2 hyperbolic intersection localization method

The initial condition for the localization are four anchors S_i with thir coordinates $\{x_i, y_i, z_i\}$ and the target S which is to be located. By multiplying relative delays by the speed of sound c

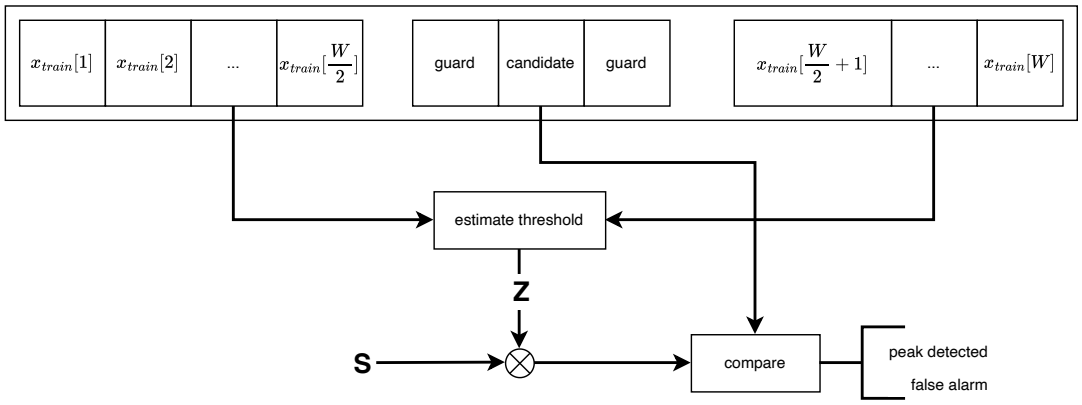

Figure 5.1: CFAR threshold peak detection procedure [Roh11]

which is approximately set to 1500 $\frac{m}{s}$, the distance d_{ij} between the reference anchor S_0 and S_i is calculated [WXX11].

$$d_{ij} = c \cdot \tau_{ij} = c \cdot (t_i - t_j), \quad \text{absolute delays } t_k,\ k \in \{0,1,2,3\} \tag{5.3}$$

$$x_{ji} := x_j - x_i, \quad y_{ji} := y_j - y_i, \quad z_{ji} := z_j - z_i \tag{5.4}$$

Every TDOA estimate creates hyperbolic curves which anchors is placed at its foci. By rearranging the derivation of hyperbola intersections the following substitutes can be defined [BM02].

$$A = \frac{d_{02}x_{10} - d_{01}x_{20}}{d_{01}y_{20} - d_{02}y_{10}}, \quad B = \frac{d_{02}z_{10} - d_{01}z_{20}}{d_{01}y_{20} - d_{02}y_{10}} \tag{5.5}$$

(The complete formula is inside the appendix)

A downside of this approach is the uncertainty of position z. Thus, additional information on bounds is necessary. The target won't get above sea level. Consequently, at least one boundary $z_{surface}$ which acts like a maximum can be set. The minimum value z_{ground} can be assumed as the lowest position achievable underwater.

$$z_{a,b} = \frac{N}{2M} \pm \sqrt{\left(\frac{N}{2M}\right)^2 - \frac{O}{M}} \tag{5.6}$$

$$z = \min\left\{\max\left\{z_a,\ z_b,\ z_{surface}\right\},\ z_{ground}\right\} \tag{5.7}$$

One other solution to this issue is to utilize information about our previous location z'. Specifically, we can calculate the distance between our current position and the two potential

candidates for the next estimate of z, and choose the candidate with the shorter distance.

$$z = \begin{cases} z_a & \text{if } |z_a - z'| < |z_b - z'| \\ z_b & \text{else} \end{cases} \tag{5.8}$$

The resulting x and y values of our target can then be calculated by the following formula using the selected z.

$$\vec{x} = \begin{bmatrix} x \\ y \\ z \end{bmatrix} = \begin{bmatrix} Gz + J \\ Iz + H \\ z \end{bmatrix} \tag{5.9}$$

5.3 Localization Simulation

In preparation for the field testing, several 3-dimensional space paths were simulated, wherein the generated points formed a helical curve that expanded in the z-direction 5.10. The positions of four anchors were utilized to calculate the TDOA values using multilateration techniques, which were subsequently incorporated into the localization algorithm 5.11. Further, an approximate value for the speed of sound c in water was used as a parameter in the calculations. Multiple runs, utilizing varying SNR's and watermark channels were conducted to evaluate the performance of the peak detection method.

$$\vec{x}_\phi(\alpha, \beta) = \begin{bmatrix} \alpha \cdot \sin\phi + \beta \\ \alpha \cdot \cos\phi + \beta \\ -|\phi| \leq z \leq -1 \end{bmatrix} \tag{5.10}$$

$$\tau_i = \frac{1}{c} \cdot (|S - S_0| - |S - S_i|) \tag{5.11}$$

5.4 Localization field testing

A field test was conducted at a shoreline location. Three hydrophones were deployed at a depth of one meter below sea level. Anchors A and B were positioned with a distance of 4.1 m between them, with Anchor B located 10.74 m from the receiving hydrophone. During the test, the underwater speed of sound, as measured using a CTD Sensor (Conductivity, Temperature, and Depth), was 1430.3 $\frac{m}{s}$. The receiving hydrophone was also relocated to a second location, 5.56 m from Anchor B.

In the first run codes of degree ten were transmitted for a total time of $50\,s$. Afterwards the receiving hydrophone was moved $5.18\,m$ further away from the anchors. Then again three test runs were done with code degrees of ten, nine and seven. Every run was repeated with a more decreased signal intensity for testing lower SNR's.

The analysis of signals generated by codes of degree ten revealed oscillating positions, with the upper and lower bounds being reached in a jumping manner. In most cases, the calculation of two distinct distances was observed, with the upper value being the more accurate representation. The lower bound may be a result of erroneous peak detection. However, slight variations in the upper positions are indicative of the true distance, which deviates by approximately $0.5\,m$ or less. These deviations can be attributed to measurement errors and the movement of the hydrophones utilized in the study because of the movement of water itself.

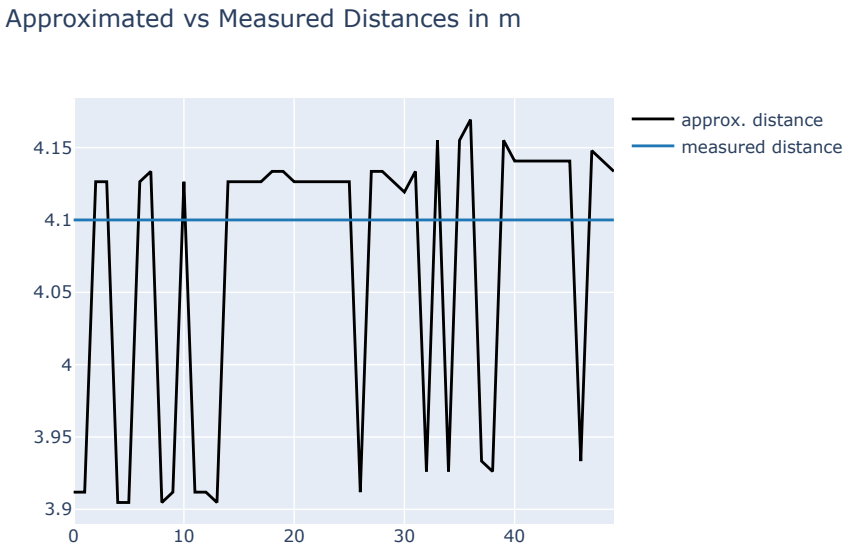

Figure 5.2: Evaluation of 10th degree code

The observed pattern is consistent across various code lengths. However, the CA-FAR false alarm rate must be adjusted for shorter code lengths due to the reduced PSR. By implementing a corrected rate and fine-tuning the threshold for peak detection, the results were found to be comparable to those obtained at other code lengths.

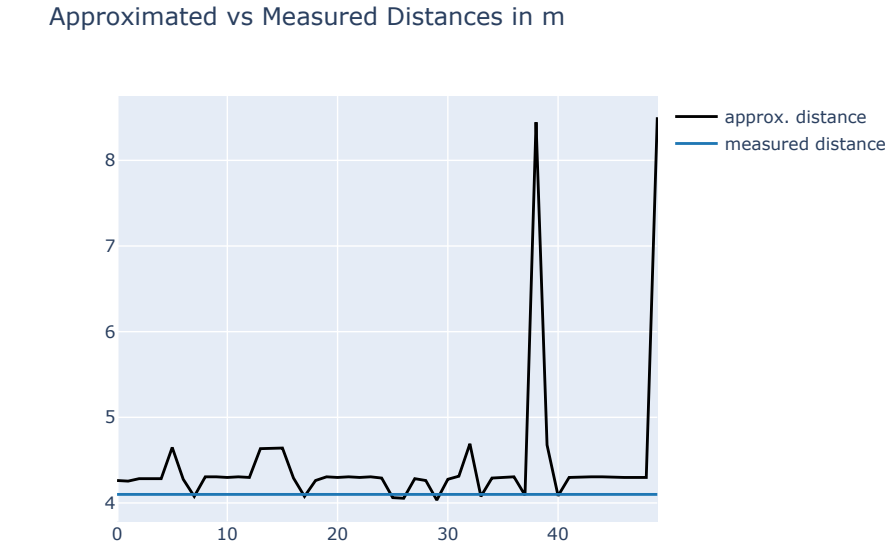

Figure 5.3: Evaluation of 10th degree code with decreased signal intensity

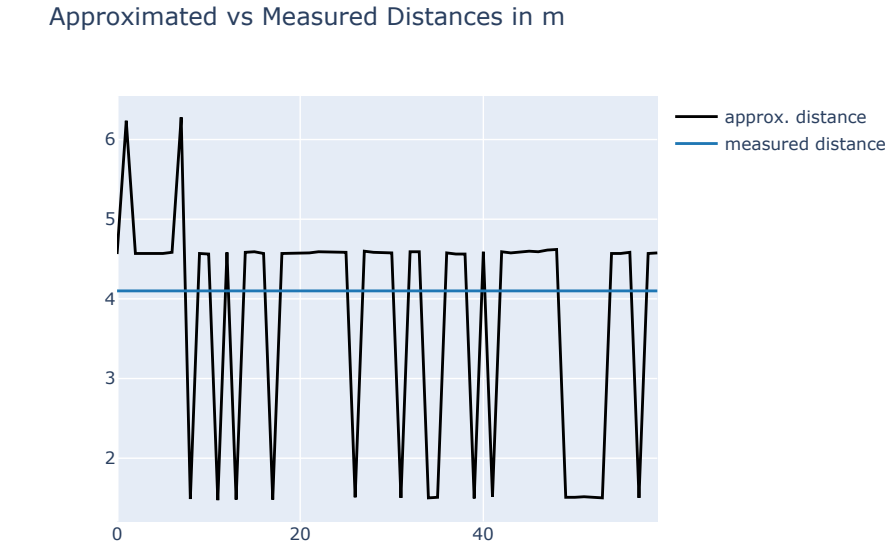

Figure 5.4: Evaluation of 10th degree code with further moved receiver

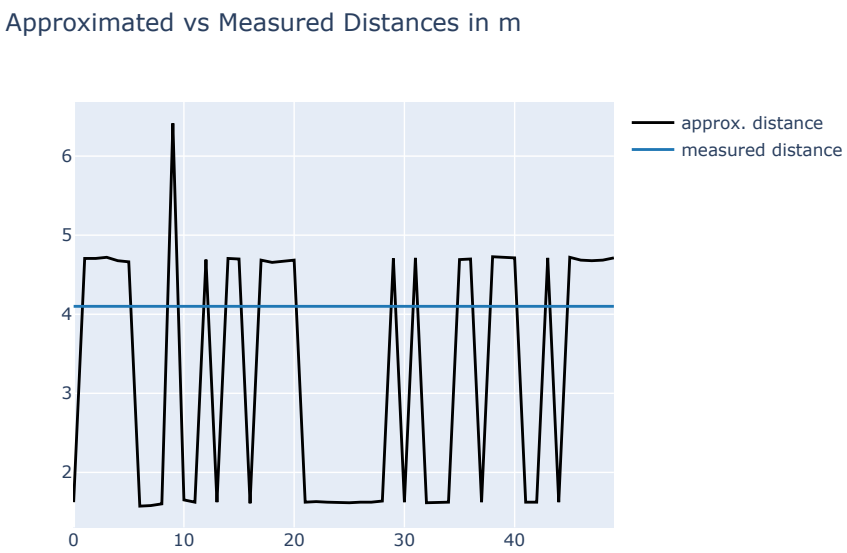

Figure 5.5: Evaluation of 10th degree code with further moved receiver and decreased signal intensity

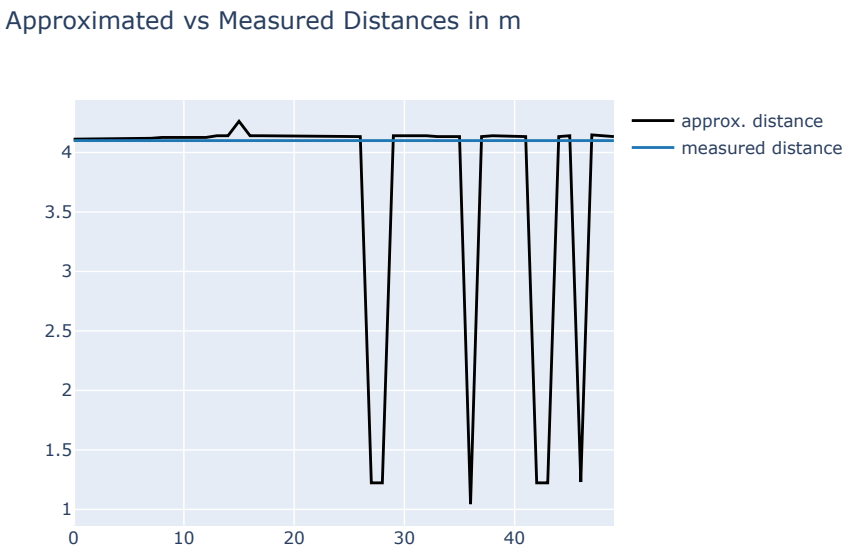

Figure 5.6: Evaluation of 9th degree code with further moved receiver

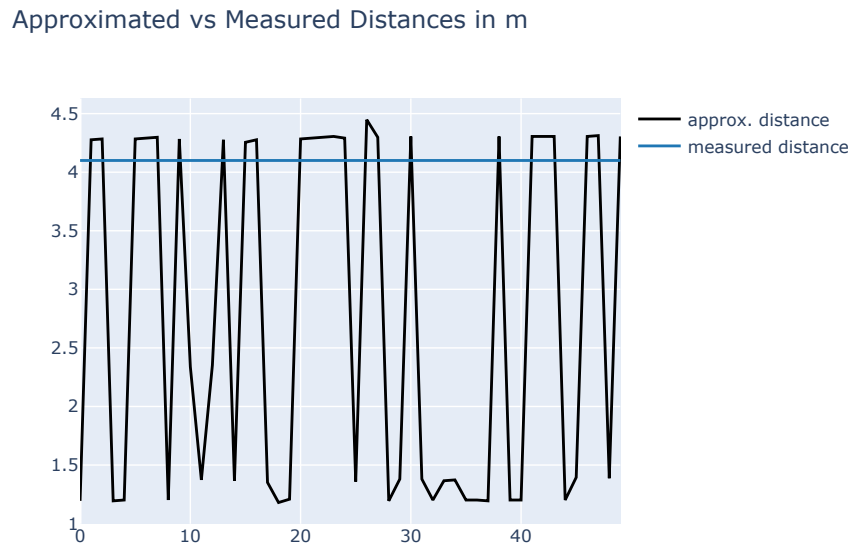

Loading [MathJax]/extensions/MathMenu.js

Figure 5.7: Evaluation of 9th degree code with further moved receiver and decreased signal intensity

Figure 5.8: location of field test, the markings represent the positions of the hydrophones. From left to right: receiver, sending anchor B and A

Bibliography

[BM02] Ralph Bucher and Durga Misra. A synthesizable vhdl model of the exact solution for three-dimensional hyperbolic positioning system. *VLSI Design*, 15, 2002.

[Gen07] Ken Gentile. Digital pulse-shaping filter basics, 2007.

[GK65] R. Gold and E. Kopitzke. Study of correlation properties of binary sequences. *Interim Tech. Rep.*, 1–4(1), 1965.

[MD] Steven J. Merrifield and John C. Devlin. The implementation of a multiplexing gold codegenerator using a xilinx logic cell array. *School of Electronic Engineering, La Trobe University*.

[PPWW72] William Wesley Peterson, Wesley Peterson, Edward J Weldon, and Edward J Weldon. *Error-correcting codes*. MIT press, 1972.

[PS08] John G. Proakis and Masoud Salehi. *Digital Communications*. McGraw-Hill Higher Education, New York, 2008.

[rad] Falschalarmrate - radar basics. https://www.radartutorial.eu/01.basics/Falschalarmrate.de.html. Accessed: 2022-11-08.

[Roh11] Hermann Rohling. Ordered statistic cfar technique - an overview. In *2011 12th International Radar Symposium (IRS)*, pages 631–638, 2011.

[SP80] Dilip V Sarwate and Michael B Pursley. Crosscorrelation properties of pseudorandom and related sequences. *Proceedings of the IEEE*, 68(5):593–619, 1980.

[vWOJ] Paul van Walree, Roald Otnes, and Trond Jenserud. Watermark.

[WXX11] Yang Weng, Wendong Xiao, and Lihua Xie. Total least squares method for robust source localization in sensor networks using tdoa measurements. *International Journal of Distributed Sensor Networks*, 7(1):172–902, 2011.

Appendix A

Content of the DVD

In this chapter, you should explain the content of your DVD.

Appendix B

Localization Formula

$$x_{ji} := x_j - x_i, \quad y_{ji} := y_j - y_i, \quad z_{ji} := z_j - z_i \tag{B.1}$$

$$A = \frac{d_{02}x_{10} - d_{01}x_{20}}{d_{01}y_{20} - d_{02}y_{10}}, \quad B = \frac{d_{02}z_{10} - d_{01}z_{20}}{d_{01}y_{20} - d_{02}y_{10}} \tag{B.2}$$

$$C = \frac{d_{02}\left(d_{01}^2 + x_0^2 - x_1^2 + y_0^2 - y_1^2 + z_0^2 - z_1^2\right) - d_{01}\left(d_{02}^2 + x_0^2 - x_2^2 + y_0^2 - y_2^2 + z_0^2 - z_2^2\right)}{2\left(d_{01}y_{20} - d_{02}y_{10}\right)} \tag{B.3}$$

$$D = \frac{d_{23}x_{12} - d_{21}x_{32}}{d_{21}y_{32} - d_{23}y_{12}}, \quad E = \frac{d_{23}z_{12} - d_{21}z_{32}}{d_{21}y_{32} - d_{23}y_{12}} \tag{B.4}$$

$$F = \frac{d_{23}\left(d_{21}^2 + x_1^2 - x_1^2 + y_1^2 - y_1^2 + z_0^2 - z_1^2\right) - d_{21}\left(d_{23}^2 + x_1^2 - x_2^2 + y_1^2 - y_2^2 + z_1^2 - z_2^2\right)}{2\left(d_{21}y_{32} - d_{23}y_{12}\right)} \tag{B.5}$$

$$G = \frac{E - B}{A - D}, \quad H = \frac{F - C}{A - D}, \quad I = A \cdot G + B, \quad J = A \cdot H + C \tag{B.6}$$

$$K = d_{02}^2 + x_0^2 - x_2^2 + y_0^2 - y_2^2 + z_0^2 - z_2^2 + 2x_{20}H + 2y_{20}J \tag{B.7}$$

$$L = 2\left(x_{20}G + y_{20}I + z_{20}\right) \tag{B.8}$$

$$M = 4d_{02}^2\left(G^2 + I^2 + 1\right) - L^2 \tag{B.9}$$

$$N = 8d_{02}^2\left[G\left(x_0 - H\right) + I\left(y_0 - J\right) + z_0\right] + 2L \cdot K \tag{B.10}$$

$$O = 4d_{02}^2 \left[(x_0 - H)^2 + (y_0 - J)^2 + z_0^2 \right] - K^2 \tag{B.11}$$

$$z_{a,b} = \frac{N}{2M} \pm \sqrt{\left(\frac{N}{2M} \right)^2 - \frac{O}{M}} \tag{B.12}$$

$$z = \min \left\{ \max \left\{ z_a,\, z_b,\, z_{surface} \right\},\, z_{ground} \right\} \tag{B.13}$$

$$z = \begin{cases} z_a & \text{if } |z_a - z'| < |z_b - z'| \\ z_b & \text{else} \end{cases} \tag{B.14}$$

$$\vec{x} = \begin{bmatrix} x \\ y \\ z \end{bmatrix} = \begin{bmatrix} Gz + J \\ Iz + H \\ z \end{bmatrix} \tag{B.15}$$